



ELSEVIER

Marine Geology 191 (2002) 1–18



www.elsevier.com/locate/margeo

Glacimarine sedimentation in Kangerdluk (Disko Fjord), West Greenland, in response to a surging glacier

Robert Gilbert^{a,*}, Niels Nielsen^b, Henrik Möller^b, Joseph R. Desloges^c, Morten Rasch^d

^a Department of Geography, Queen's University, Kingston, ON, Canada K7L 3N6

^b Institute of Geography, University of Copenhagen, Øster Voldgade 10, 1350 Copenhagen, Denmark

^c Department of Geography, University of Toronto, Toronto, ON, Canada M5S 3G3

^d Danish Polar Centre, Strandgade 100H, 1401 Copenhagen, Denmark

Received 12 December 2001; accepted 30 August 2002

Abstract

Beginning in 1995, a large outlet glacier of the Sermersauq Ice Cap on Disko Island surged 10.5 km downvalley to within 10 km of the head of the fjord, Kuannersuit Sulluat, reaching its maximum extent in summer 1999 before beginning to retreat. Sediment discharge to the fjord increased from 13×10^3 t day⁻¹ in 1997 to 38×10^3 t day⁻¹ in 1999. CTD results, sediment traps and cores from the 2000 melt season document the impact of the surge on the glacimarine environment of the fjord. Within 4 km of the inflow sedimentation rates increased by 30 times over those before the surge, reaching an estimated maximum value of 29 cm a⁻¹ (up to 4.2 mm day⁻¹ between 24 July and 9 September 2000). Fine-grained deposits from suspension in the water column displayed diurnal laminations in response to the interaction of tidal cycles with the sediment plume; these are not found in the sediments deposited before surging. Thin beds of sandy turbidites from turbidity currents originating from slope failures on the delta front occurred at about 20 day intervals during the melt season. Each of these effects was limited to within several kilometres of the point of inflow, but provide a unique signal significantly different from those generated by normal hydroclimatically induced events.

© 2002 Elsevier Science B.V. All rights reserved.

Keywords: glacimarine; sediment; fjord; Greenland; glacier surge

1. Introduction

Since we carried out studies of the inner portions of fjords on Disko Island, West Greenland

(Fig. 1) in 1995, including the northeast arm of Kangerdluk (Disko Fjord) called Kuannersuit Sulluat (Gilbert et al., 1998), an outlet glacier of the Sermersauq Ice Cap has surged 10.5 km downvalley to within 10 km of the fjord. We hypothesised that this event would create a distinct glacimarine sedimentary record in the fjord because surging represents a major disruption to the glacier. Thus, sediment production from the glacier and from the land overridden and exposed

* Corresponding author. Fax: +1-613-533-6122.
E-mail address: gilbert@lake.geog.queensu.ca
(R. Gilbert).

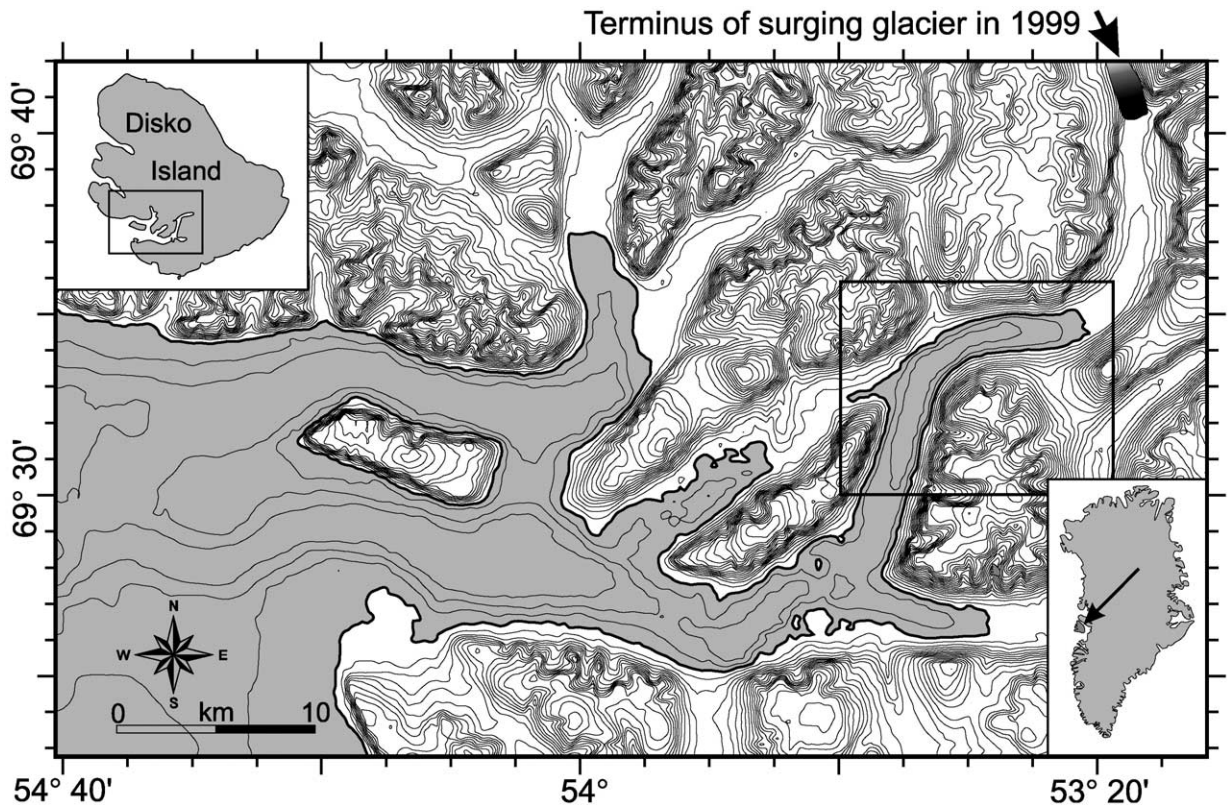


Fig. 1. Location of Kangerdluk (Disko Fjord) on Disko Island, West Greenland, showing the terminus of the surging glacier at maximum extent. Isobaths and contours are at 50 m intervals below and above sea level (shaded), respectively. The box outlines Kuannersuit Sulluat as shown in Figs. 3, 11 and 12. Insets illustrate Disko Island and Greenland.

during rapid advance and subsequent wasting (Sharp, 1988) should increase significantly. Surging is a short-lived phenomenon normally lasting several years (Dowdeswell et al., 1991) which occurs between decades to centuries of quiescence and is largely independent of climatic controls (Meier and Post, 1969; Raymond, 1987), including year-to-year fluctuations in temperature or precipitation, and accumulation and ablation. Thus, distinguishing the stratigraphic character of its sedimentary deposits from those of hydroclimatically induced events (particularly floods due to glacier melting during warm periods, and to major rain storms) is potentially important when using glacial marine sediments for palaeoenvironmental assessment. The impact of glacial surging on the glacial marine depositional environment has been investigated previously in Alaska by

Jaeger and Nittrouer (1999a) and in Svalbard by Solheim and Pfirman (1985).

This paper reports observations of the record of the surge in the sediments of Kuannersuit Sulluat in comparison to the environment before the surge. We assess whether the record of this event is distinctive, and whether it can be distinguished from hydroclimatically controlled sedimentation. Background on the hydrology, climate, oceanography, glacial history, and landscape of the region is provided by Gilbert et al. (1998) and Desloges et al. (2002).

2. The glacial surge

The glacier is not visible from the fjord, and the land above the head of the fjord is unoccupied

and flown over infrequently. Thus, surging of the glacier, begun in 1995, was undetected until July 1999, when it was discovered during a geomorphic survey of the valley. Mapping from TM, Landsat and SPOT satellite imagery, and subsequent field work have documented the history of the event. On 17 June 1995 the terminus of the glacier was about where it appears in the 1985 air photography (Fig. 2). By 24 September 1995 the glacier had advanced 1.25 km and by 12 October another 1.25 km (mean advance during the second period: 70 m day⁻¹). The advance slowed from 18 m day⁻¹ in 1996 to 5 m day⁻¹ in 1997 and <1 m day⁻¹ between 1997 and 1999. By summer 1999 the advance ceased; the maximum extension of the terminus, about 10.5 km down-valley to about 10 km from the head of the fjord, was mapped from imagery on 9 July 1999 (Fig. 2). Subsequently, the glacier began to retreat. The tongue of the glacier averages 0.7 km wide and 250–300 m thick, representing 2 km³ of ice transported from the Sermerssuaq Ice Cap (about 1400 m a.s.l.) to the valley at 100–200 m a.s.l. (Fig. 1). A terminal moraine, 30–40 m high, has formed in front of the glacier.

Spot measurements of water and sediment discharge were made at and near the glacier terminus, and on the sandur about 8 km downstream from the glacier. Maximum discharge was about 100 m³ s⁻¹ during peak glacial melt in July 1999 and 2001, and from 35 to 40 m³ s⁻¹ in 1997 and 2000. In July 1999 concentration of suspended sediment was measured at 11.5 g l⁻¹ at the glacier terminus, decreasing to 8.1 g l⁻¹ 2.1 km down-valley, and 4.1 g l⁻¹ at the sandur station. These values are greater than in most arctic proglacial rivers but are comparable to maximum concentrations in alpine glacial streams, even associated with jökulhlaups. However, they are significantly below the highest values in high energy glacial streams in temperate regions where concentrations up to 80 g l⁻¹ have been recorded (Gilbert, 2000 Fig. 6). Mean grain size of the suspended sediment decreased from 133 µm at the terminus to 111 µm 2.1 km from the glacier, and 87 µm 8 km from the glacier.

Substantial amounts of fine-grained suspended sediment were deposited on the sandur between

the glacier and the fjord. Nevertheless, it is estimated that 13 × 10³ t day⁻¹ was delivered to the fjord during the 1997 melt season and 38 × 10³ t day⁻¹ was delivered in 1999.

3. Methods

During the summer of 2000, working from the 15 m research vessel, *Porsild*, an acoustic survey of the fjord was conducted using a CHIRP sub-bottom profiling system. Paired, cylindrical sediment traps (inside diameter, 8 cm; height, 40 cm) were deployed from 10 June to 23 July and from 24 July to 9 September 2000 at several locations in the upper fjord (Fig. 3). Traps were located 5, 10 and 40 m above the sea floor. Sediment recovered was washed into Nalgene bottles on site and thoroughly mixed before laboratory analyses. Short gravity cores were taken and CTD profiles were recorded at stations throughout Kuannersuit Sulluat (Fig. 3). Positions located by GPS are accurate to ±10 m or less. The stream flowing over the sandur to the head of the fjord was gauged and integrated suspended sediment samples were recovered from primary channels.

In the laboratory the mass of dried sediment from the traps was recorded. Representative samples were analysed for organic matter by loss-on-ignition (LOI) at 550°C and grain size using a Malvern laser diffraction instrument. Volumetric accumulation rates (mm day⁻¹) were calculated from the mass accumulation rates (g cm⁻¹ day⁻¹) using the mean bulk density (1.6 g cm⁻³) of sediment in the top 0.5 m of cores from the trap sites. The cores were photographed, X-rayed and logged. X-radiographs provided measures of the number and size of gravel particles interpreted as ice-rafted debris (IRD) and the grey-scale (GS) of the scanned images was plotted as a measure of the properties of the sand and silt. Magnetic susceptibility (MS) was measured at 3 mm intervals with a high-resolution Bartington instrument, using an automated Tamiscan stage. Grain size finer than 2 mm was determined using a Coulter laser diffraction instrument, and organic matter and carbonate was measured by LOI at 550 and 1000°C, respectively.



4. Sediment routing

CTD profiles document the distribution of sediment from the sandur in the water of Kuannersuit Sulluat (Fig. 3a,b). A cap of brackish water about 2–4 m thick with salinity 15–20‰ indicates significant mixing of sea water (33–33.5‰) across the pycnocline everywhere in the fjord. Water temperature decreases from 10–12°C in the cap to –0.5 to –0.8°C at about 30 m depth, below which it remains almost constant to the bottom.

The suspended sediment concentration (SSC) near the surface is 40–100 mg l⁻¹ near the delta, decreasing to 5–30 mg l⁻¹ within about 5 km downfjord. These concentrations are significantly lower than those measured in the river due to settling of most of the sand and coarse silt at the distributary mouths and scavenging of the finer sediments by flocculation from the water column.

At several locations within 2 km of the delta, higher SSC was recorded along the sea floor. Although SSC measured on the sandur was much below the 38 g l⁻¹ necessary to generate turbidity currents directly from inflow (Gilbert, 1983), the elevated SSC at the sea floor may be caused by turbidity currents due to small slumps below the pycnocline on the rapidly oversteepening distributary mouths. Detail of the CTD near the sea floor at site 4 (Fig. 4) shows an anomaly below 67 m depth, about 7 m above the sea floor, where the water is slightly warmer and less saline, suggesting an origin in shallower water, about 20–40 m depth (compare Fig. 3a). SSC up to 160 mg l⁻¹ allows this layer to have slightly greater density than the water above. Calculation based on the Middleton (1966) equation for the velocity of uniform flow in a turbidity current indicates a mean velocity of 4 cm s⁻¹ and a densitometric Froude number of 0.7 assuming a small density difference of 0.05 g l⁻¹ between the current and the ambient fluid (Fig. 4). This current is capable

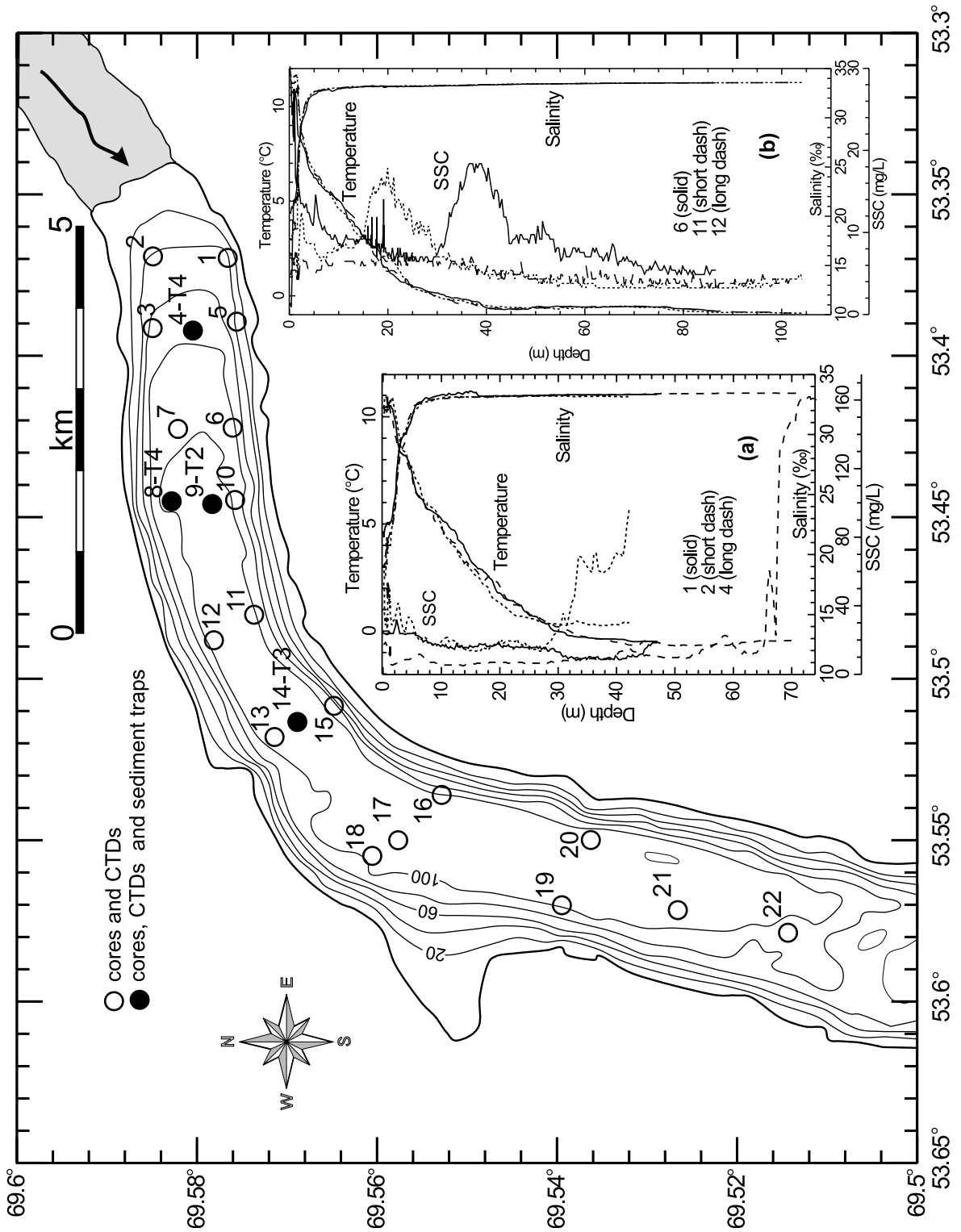
of transporting fine and medium sand but would be unable to erode sediment from the sea floor. The small density difference gives rise to a Froude number close to 1 and so mixing across the interface is probable (Gilbert, 2000, Fig. 3), reducing the sediment concentration and thus density, and slowing and dissipating the current.

Supporting the interpretation of turbidity currents was the presence of 1–2 m willow trees (*Salix* sp.) complete with root systems commonly found wrapped around the anchors of the sediment traps when they were retrieved after the first deployment. These were probably ripped up during the advance of the surging glacier, transported to the fjord, buried and water-logged in the sediment on the delta foreset beds, to be released by failure and transported in the intermittent turbidity currents.

Beyond about 3 km from the head of the fjord, turbidity currents were not recorded. Rather, at some sites a weakly turbid plume (SSC < 20 mg l⁻¹) was observed as interflow about 20 and 40 m depth, within and near the base of the zone of decreasing temperature. SSC plays a very minor role in determining the density of this water. For example, between 30 and 45 m depth at site 6 (Fig. 3b) the density increase due to salinity and temperature is 0.201 g l⁻¹; SSC at the maximum concentration in the plume (19 mg l⁻¹) increases density by 0.012 g l⁻¹. These plumes may represent turbidity currents in shallower water lifting off the sea floor to become interflow, or more likely, plumes settling from above (cf. Mackiewicz et al., 1984; Cowan et al., 1998). Although the temperature and salinity profiles were similar everywhere in the study region (Fig. 3a,b), by about 7 km from the delta, turbid plumes had disappeared completely and SSC was uniformly less than about 5 mg l⁻¹.

The trapped sediment masses document rates of accumulation ranging from 0.01 to 0.34 g cm⁻² day⁻¹ in the first deployment period and from

Fig. 2. Tuned orthophotograph from original air photograph taken in July 1985 (source: Kort- og Matrikelstyrelsen Flight 886F, No. 2666 copyright) showing the position of the glacier 10 years before surging. Superimposed are the locations of the ice mapped from TM, SPOT and Landsat imagery: (1) 17 June 1995, (2) 24 September 1995, (3) 20 October 1995, (4) 20 May 1996, (5) 22 September 1996, (6) 24 September 1997, (7) 9 July 1999, and (8) 30 September 1999.



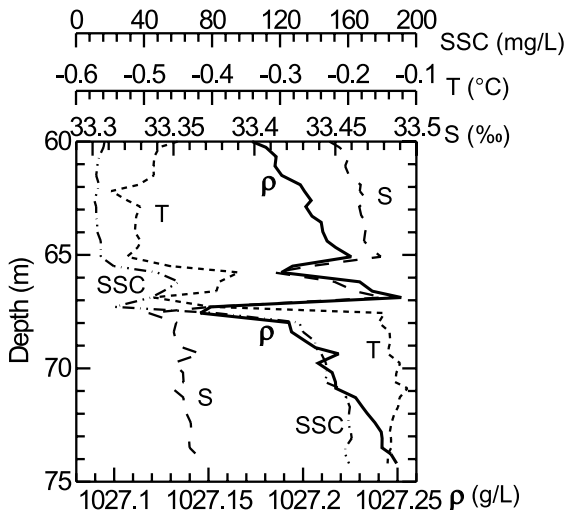


Fig. 4. Detail of the CTD cast near the sea floor at site 4 (Fig. 3) showing suspended sediment concentration (SSC) determined as indicated in Fig. 3, temperature (T), salinity (S) and density (ρ) determined from the other parameters.

0.02 to $0.67 \text{ g cm}^{-2} \text{ day}^{-1}$ in the second period (Fig. 5). The rates are highest near the delta and decline significantly downfjord (compare the CTD results) as reported elsewhere (e.g. Syvitski et al., 1987). Compared with most other fjord environments (Jaeger and Nittrouer, 1999b) the rates are very high. Accumulation also increases with depth at all locations in response to the larger water column contributing more sediment over successively deeper traps, and the occurrence of turbidity currents on the sea floor (for example, the lowest traps, 5 m above the bottom would be within the upper part of the turbidity current shown in Fig. 4). At proximal site T1 the rates in the traps higher in the water column were greater during the second period, reflecting the charging of the water mass by suspended sediment. At sites T2 and T3 the rates were approximately the same during the second period. Although the discharge from glacial melt declined

during the second period, three major storms occurred in this period with 70, 105 and 87 mm of rainfall, respectively (total rainfall in the first period was 29 mm). A large subaerial mudslide induced by the second event occurred on the valley side close to the delta front, contributing a significant pulse of sediment to the sandur.

The particle-size distributions (PSDs) shown in Fig. 6 of the trapped sediment also document the sedimentary processes. At all sites the differences between traps at the same location are very small and within analytical error, suggesting consistent capture of the ambient sedimentary environment. In the first deployment period (Fig. 6a), sediment in the lower traps at the proximal sites T1 and T2 contains up to 35–64% sand with mean grain size in the fine sand range (the mean grain size of the suspended sediment was $87 \mu\text{m}$ on the sandur about 2 km from the fjord), whereas at T1 the upper two traps contained almost no sand. This corresponds with the observation of turbidity currents reported above and sandy laminae in the cores reported below. The trap at 10 m above the sea floor at T2 contained sediment of almost identical grain size as the lower trap, suggesting that the turbidity currents at this location were thicker and transported sediment well mixed through at least 10 m depth (cf. Bornhold et al., 1994; Jaeger and Nittrouer, 1999b). It is curious that the trap 10 m above the sea floor contained a small secondary mode in the coarse sand to fine gravel range. Sea ice had melted by the time the traps were deployed, so ice rafting may be discounted. This sediment must have reached this site by a large turbidity current capable of transporting this sediment at least 10 m off the sea floor. Curious as well is the significant sand component (17%) in the upper trap at T2, 40 m above the sea floor. The settling velocity of the coarsest of this sediment is about 5 cm s^{-1} and it is difficult to imagine it being transported so far from

Fig. 3. Kuannersuit Sulluat showing sampling locations. Numbers refer to cores (prefixed by 'D' elsewhere in this paper) and CTD casts; numbers prefixed by 'T' refer to trap sets. Inset graphs show selected CTD results on 25 July 2000 from sites (a) 1, 2 and 4, and (b) 6, 11 and 12. Suspended sediment concentration (SSC in mg l^{-1}) was determined from backscatter, B , in FTU as $\text{SSC} = 1.1067B$, $r^2 = 0.99$ by calibration with 13 in situ water samples filtered at $0.7 \mu\text{m}$ and ignited at 550°C to remove organic matter.

the delta by overflow or interflow. The secondary mode in most of these distributions in the silt and clay size range indicates the separate process of settling from suspension of sediment in the water column.

During the second deployment period (Fig. 6b), which occurred after the cores described below were recovered, PSD at all sites and at all depths was very similar with mean grain size in the mid silt range and only a small fraction of sand (0–6%).

The organic matter content of the trapped sediment is plotted in Fig. 7. Content varies from 2 to 6% with the higher values in the second period as the clastic component decreased.

Annual accumulation rates at the core sites have been calculated from the trap data, assuming a small input in the melt season before and after the traps were deployed and during the winter period. The annual accumulation rate at T1 (2 km) is 29 cm a^{-1} , with a small decline to 27 cm a^{-1} at T2 (4 km) but very much lower at 3.0 cm a^{-1} at T3 (7 km). Mean net accumulation rate for the 8.4 km^2 region covered by the sediment traps is 20 cm a^{-1} . These rates compare well

with the 0.1 cm day^{-1} reported by Jaeger and Nittrouer (1999a) associated with the surging of the Bering Glacier, Alaska.

5. Sedimentary record

The cores (Fig. 8) record the effects of the surge in Kuannersuit Sulluat. The proximal environment within 2 km of the sandur is represented by core D4 in which the fine-grained sediments are well-laminated (Fig. 9), indicating discrete, episodic events of deposition (Ó Cofaigh and Dowdeswell, 2001). These sediments have mean grain size of $6\text{--}10 \mu\text{m}$, and the distributions are unimodal and exhibit weak negative (coarse tail) skewness, with little or no sand present (Fig. 10b,c). These values correspond with the PSD recorded in the upper traps (compare Figs. 6 and 10), indicating the predominance of deposition from suspension in the water column. The thickness of the laminae varies from less than 1 to about 3 mm, suggesting, based on the accumulation of 2.1 mm day^{-1} in traps T1 and T2 (Fig. 5), that the cyclic depositional events occur on aver-

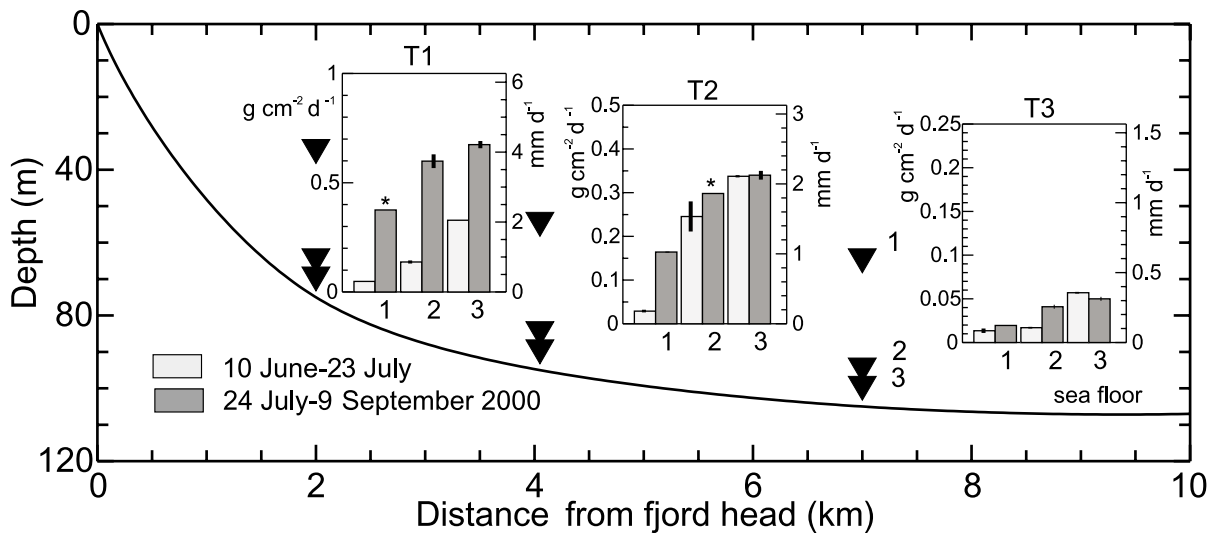


Fig. 5. Mass ($\text{g cm}^{-2} \text{ day}^{-1}$) and volume (mm day^{-1}) accumulation rates in sediment traps (shown as triangles) during two periods in summer 2000. Volume rates are based on mean bulk density of 1.6 g cm^{-3} in the upper parts of cores from the region. Numbers refer to trap pairs at (1) 40 m, (2) 10 m, and (3) 5 m above the sea floor. Shaded bars show the mean accumulation from two traps at the same location. Small bars show the range except where data from only one trap were available (indicated by an asterisk). Where error bars do not appear, they are smaller than the line thickness of the shaded bars. Note the scales of the abscissae double downfjord between successive graphs.

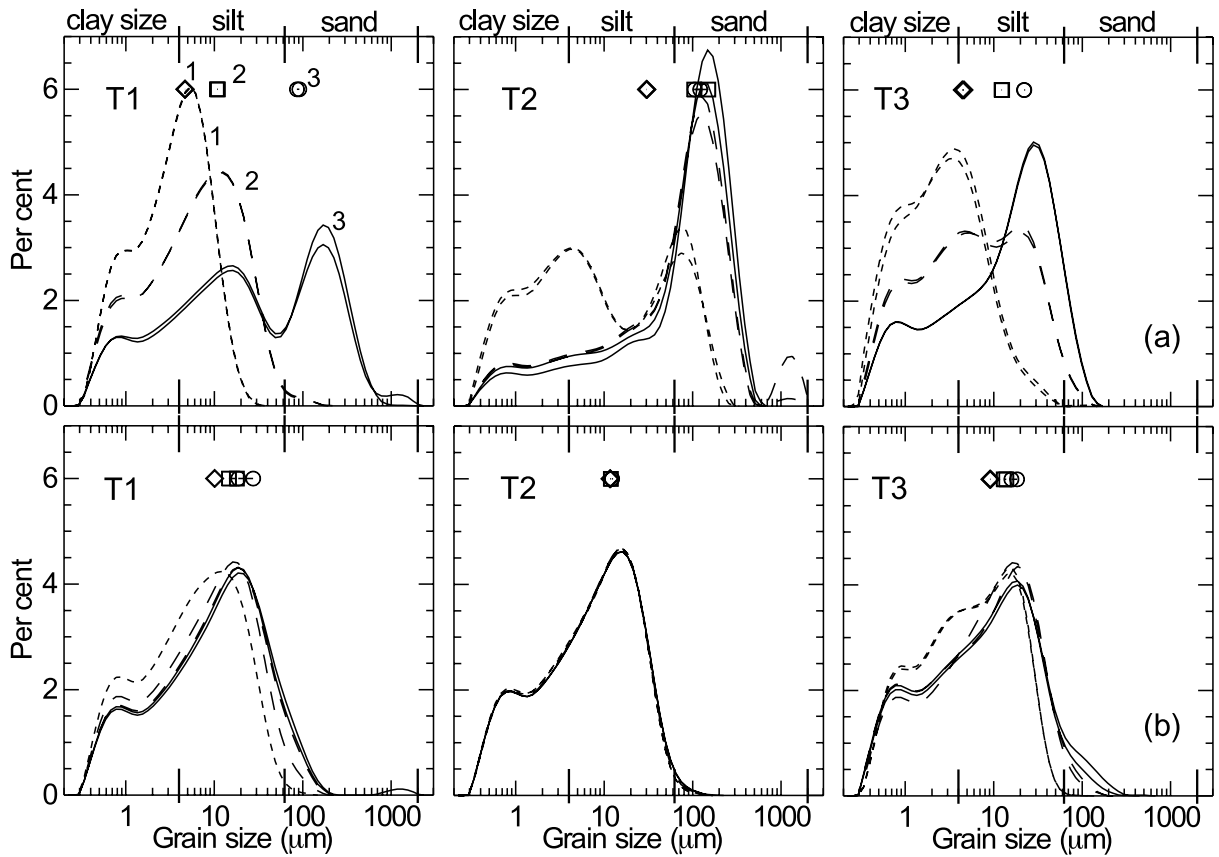


Fig. 6. Particle-size distributions of sediment trapped during (a) 10 June to 23 July, and (b) 24 July to 9 September 2000. Symbols refer to the mean grain size. Traps are numbered as shown in Fig. 5. One sample from each of the two traps at each location is shown except T1-1 and T2-2 during the second period when sediment from only one trap was available. For locations, see Fig. 3.

age once per day, related to the diurnal fluctuation in inflow which peaked after midnight on most warm, clear days associated with glacial melt the preceding day. Field sketches made on the hill side overlooking the fjord confirmed the spreading of the plume downfjord during these nights. This suggests that the semi-diurnal tides (mean range 1.1 m) played a lesser role in the spreading of the plume than the pattern of inflow (cf. Cowan et al., 1998, 1999). However, it is probable that when ebbing tide corresponds with the daily peak inflow and with downvalley winds, the plume spreads more rapidly downfjord and carries greater sediment loads, probably contributing to thicker and more prominent laminae.

Thin, ungraded layers of muddy sand occur

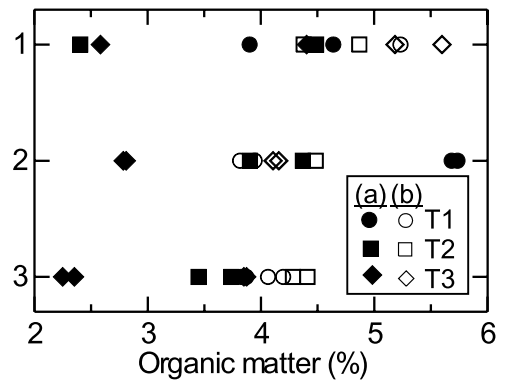


Fig. 7. Organic matter content determined by loss-on-ignition in sediment traps during the period (a) 10 June to 23 July, and (b) 24 July to 9 September 2000. Numbers on the abscissa refer to traps as shown in Fig. 5.

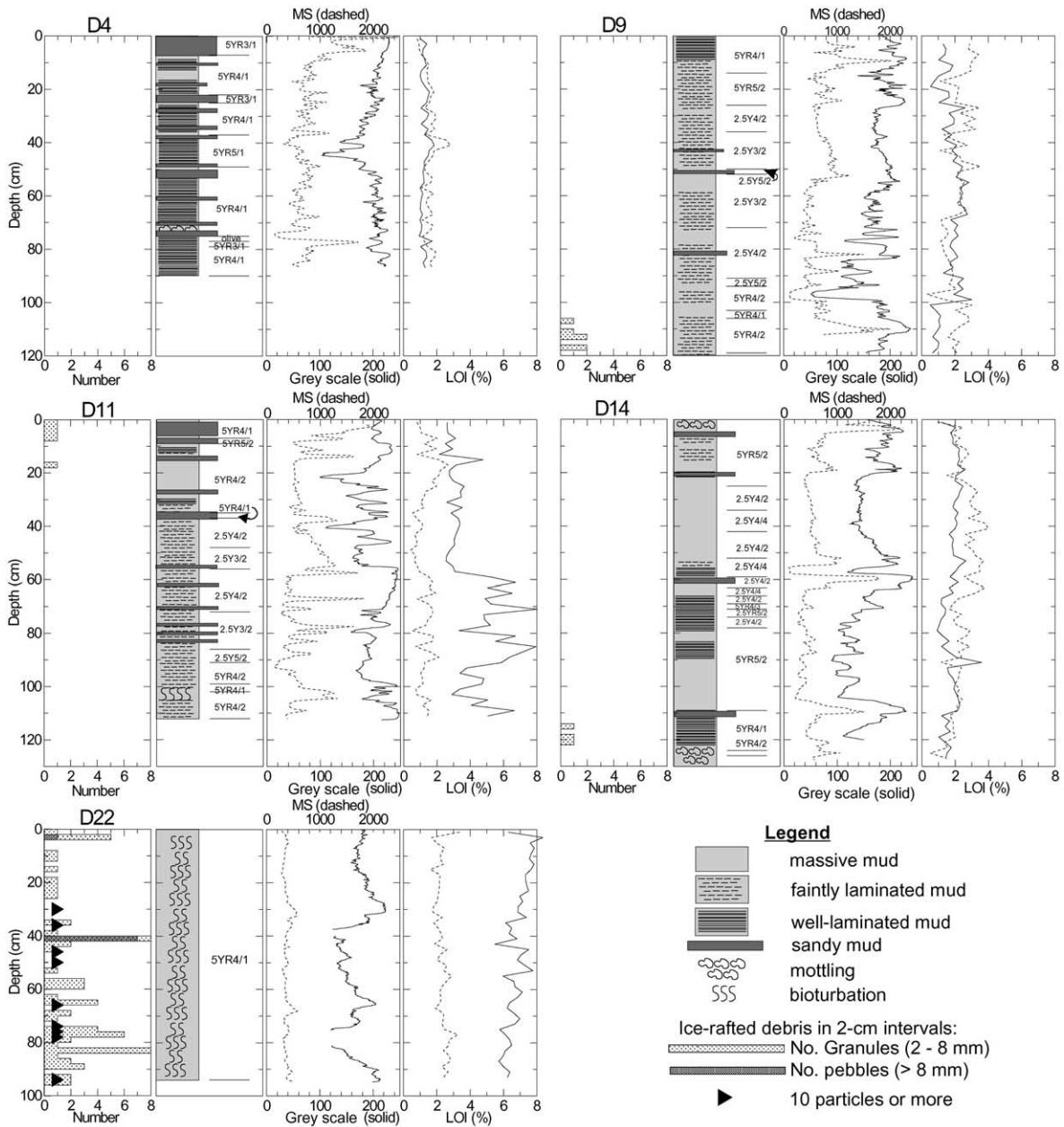


Fig. 8. Logs of selected cores from Kuannersuit Sulluat (locations in Fig. 3) showing the presence of coarse particles inferred to be ice-rafted, stratigraphy, grey scale (GS) of a 1 cm wide band of the negative X-radiographs in 0.3 mm intervals in scale from 0 (black, indicating high penetration of X-rays through fine, water-laden sediment) to 256 (white, indicating minimal penetration), magnetic susceptibility (SI) at 2 mm intervals, and loss on ignition (LOI) at 500°C, representing organic matter (solid line), and 1000°C, representing inorganic carbon (dashed line). Scales for each core are the same.

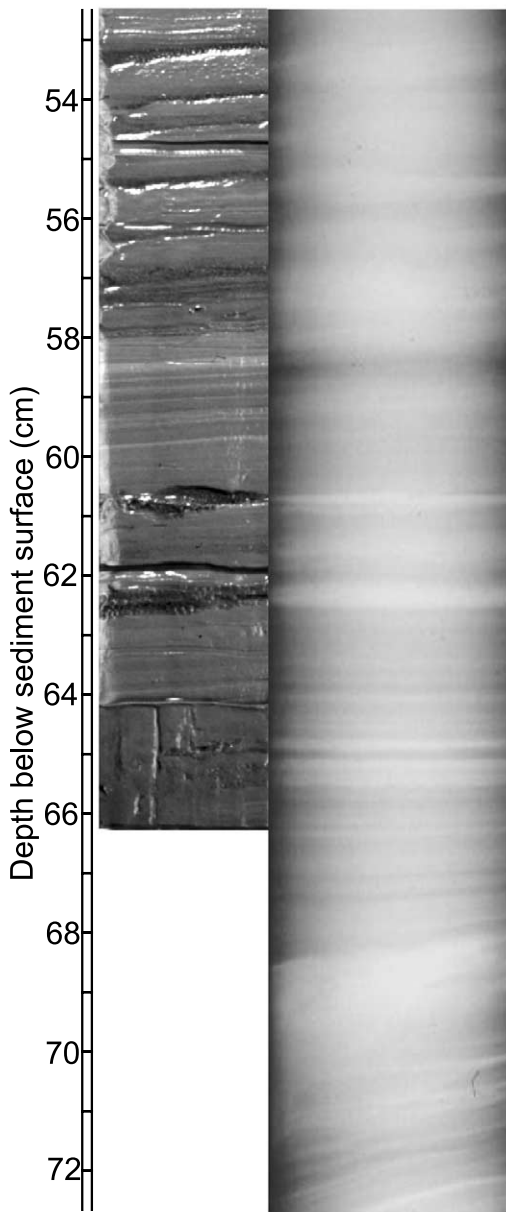


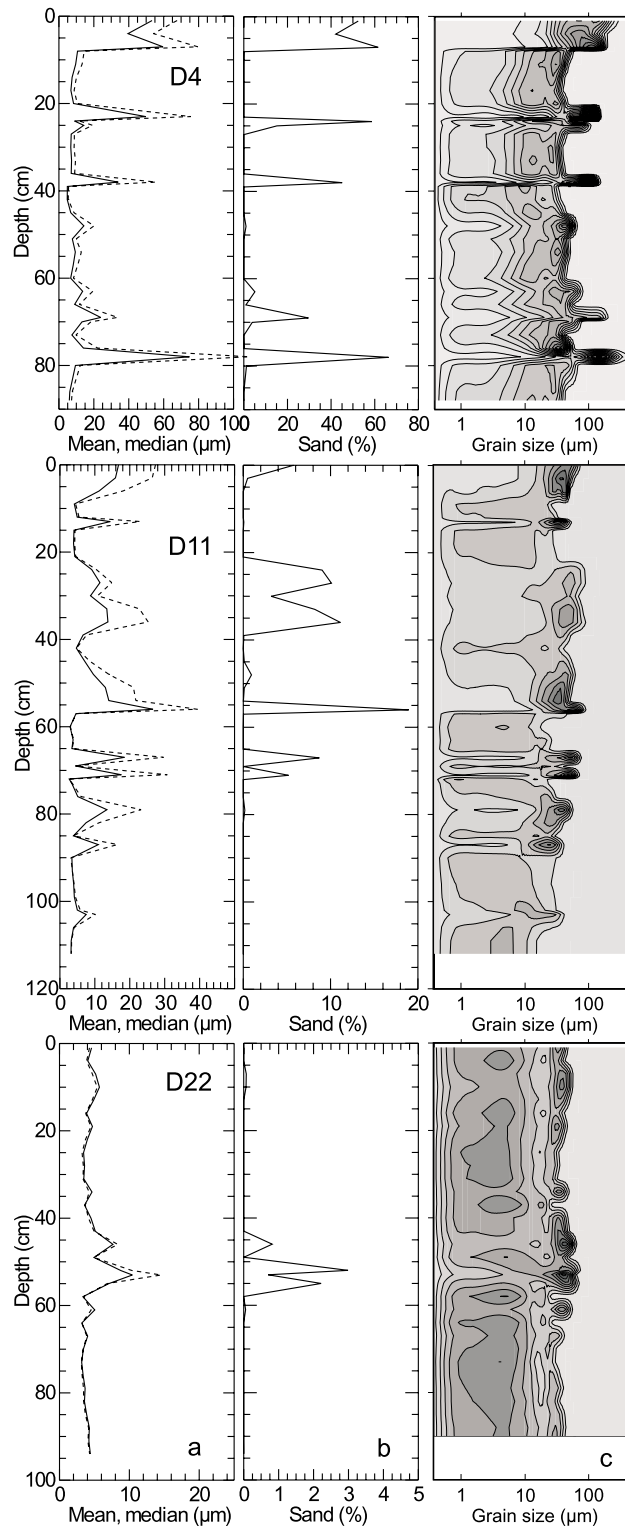
Fig. 9. Photograph and X-radiograph of part of core D4 illustrating fine laminations.

commonly in the proximal cores. Mean grain size is in the fine sand size range (50–60% sand; cf. Fig. 6) and the distributions are more strongly negatively skewed (Fig. 10). These probably indicate turbidity currents created by frequent failures on the foreset slopes. The twelve layers in core D4

(Fig. 8) suggest a mean period of about 20 days for these events based on the accumulation rates in the traps (Fig. 5). In general, these layers have both higher MS and X-radiographs have lighter toned GS, the former related to lower water content and the latter also related to greater absorption of X-rays by the larger rock and mineral fragments. Also, MS and GS show smaller layers, intermediate with the lamination in the fine sediments, which are not evident in the visual core logs. There is little or no bioturbation of the sediments in this proximal region, indicating that the benthos has been overwhelmed by the high rates of clastic accumulation (Jaeger and Nittrouer, 1999a). The fraction of organic matter based on LOI_{550} is about 1–2%, which is significantly lower than in the sediment in the water column (Fig. 7), indicating preferential deposition of clastic material in the proximal environment, or that carbon is quickly remobilised from the recently deposited sediments.

Between 4–8 km from the fjord head (represented by cores D9, D11, and D14: Fig. 8) the fine-grained sediments are weakly laminated to massive, although the grain size is comparable to the proximal sediments (Fig. 10). Rates of accumulation are much lower (Fig. 5) and only the stronger pulses associated with tidal and wind forcing in combination with the timing of the diurnal fluctuation in inflow may be registered. There is more bioturbation, both as trace fossils and as mottling, especially beyond 5 km down-fjord. The organic matter content is still low, although in some cores such as D11 it shows an increase from 3 to 5% above 60 cm depth and up to 8% below (cf. Fig. 7).

The sandy layers are less frequent, thinner, and significantly more muddy (sand content < 20%: Fig. 10), indicating that about one weak turbidity current event per year reaches this region of the fjord. This corresponds with the CTD observations reported above of the loss of elevated turbidity near the sea floor in this region. Turbidity currents are slowed both by the loss of their suspended sediment load and the low slope of the sea floor in this region beyond the foreset slopes of the delta (Fig. 3). However, the acoustic data (Fig. 11) show that ponded sediments occur dis-



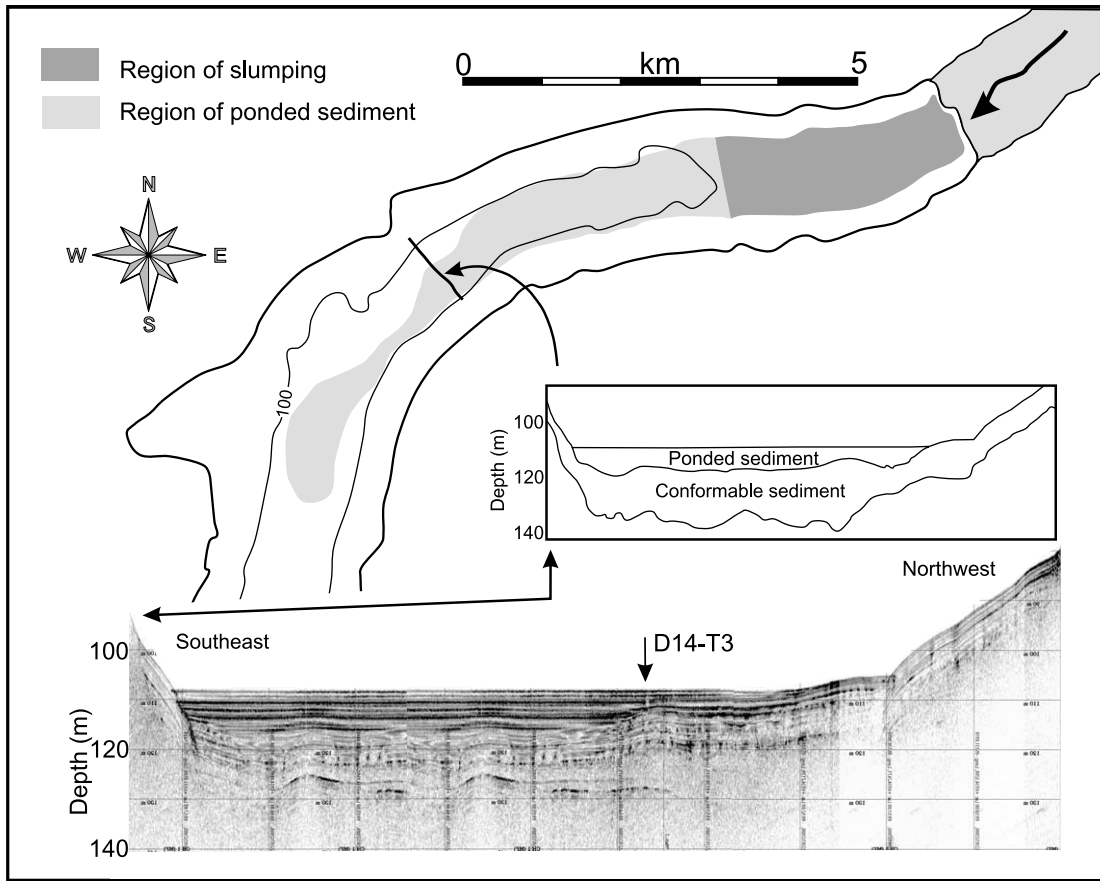


Fig. 11. Subbottom acoustic profile across the fjord illustrating conformable sedimentary deposits overlain by ponded sediments due to turbidity currents representing advance of the delta front over time. View is downfjord. Map shows the extent of the regions of slumped and ponded sediment with respect to the 100 m isobath.

tally from a zone of slumped sediments on the delta foreset zone to about 9 km downfjord from the head. They are thickest (up to 40 m) proximally where they cover the entire floor of the fjord, thinning to a few metres distally where they infill small depressions on the floor. They overlie conformable sediments on the fjord floor, overwhelming and flattening relief there. The conformable sediments are ascribed to processes dominated by spatially homogeneous settling from suspension, while the ponded sediments in-

clude a significant component of deposition from gravity flows, especially turbidity currents (Syvitski et al., 1987; Gilbert et al., 1998). We suggest that these range from more frequent low-concentration events described above arising from small slope failures and limited to the slopes of the foreset region to less frequent, more powerful events able, by inertia, to transport sand several kilometres over the flat floor of the fjord, to the largest events that pass up to 9 km downfjord. These events are not unique to the period of surg-

Fig. 10. Grain size in 2 cm intervals (closer at stratigraphic transitions – Fig. 8) of selected cores (locations in Fig. 3) excluding the IRD documented in Fig. 12, shown as (a) mean (solid line) and median (dashed line), (b) sand fraction, and (c) particle size distributions (Beierle et al., 2002). Scales vary from core to core. Isoleths in (c) represent 1% increments of sediment in 0.5 ϕ classes.

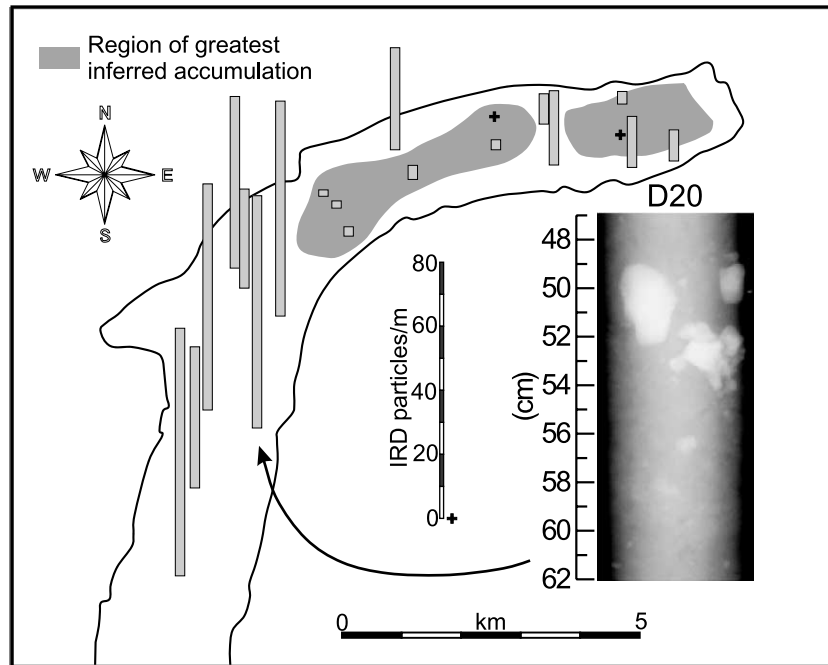


Fig. 12. Concentration of gravel particles (>2 mm diameter – Fig. 8) assessed from X-radiographs (inset shows example from core D20) inferred to be dominantly ice-rafted. Cores with low concentrations represent areas overwhelmed by fine-grained sediments delivered from the sandur.

ing but appear to be significantly more common then.

The presence of gravel (particles larger than 2 mm diameter) in the cores (Fig. 8) also indicates the nature of the sedimentary processes in the fjord. These occur as individuals or, less commonly, groups of several to a dozen or more. Given this pattern and that they are distinctly larger than the rest of the sediment, we infer that they are IRD from the shores around the fjord where they are frozen in during ice formation, and to a lesser extent loaded passively on the ice by aeolian (Gilbert, 1982; Lewis et al., 2002) and subaerial colluvial processes. It is unlikely that the IRD originated from ice bergs (cf. Ó Cofaigh et al., 2001), because, although there is a large flux along western Disko Island from major sources in Disko Bugt, they rarely penetrate the inner parts of the fjords (Gilbert et al., 1998; Desloges et al., 2002). IRD is almost absent on the fjord floor toward the head of the fjord (Fig. 8) for three reasons: (a) the high rates of deposition from the water column and by gravity flow

processes overwhelm the rate of IRD deposition, (b) persistent outflow, aided by frequent katabatic winds, pushes ice downfjord and so there is less chance to release IRD in the proximal zone, and (3) ice remains in the inner fjord longer than elsewhere, briefly preventing floating ice pans from entering this region.

When the presence of IRD is standardised to the number of particles per metre depth of sediment (where necessary by extrapolating the shorter core data: Fig. 12) a clear pattern emerges. Within 8 km of the fjord head IRD is absent or present in low concentrations. In this region the concentrations are lowest on the fjord floor, where the ponded deposits from gravity flow are greater, and are somewhat higher on the fjord side walls, where only conformable deposition from suspension occurs. The proximity to the sources along the shores may also contribute the higher concentrations on the side walls. The reason for the slightly higher concentrations in two cores on the fjord floor 3 km from the delta is unknown; this may just be an artifact of the qua-

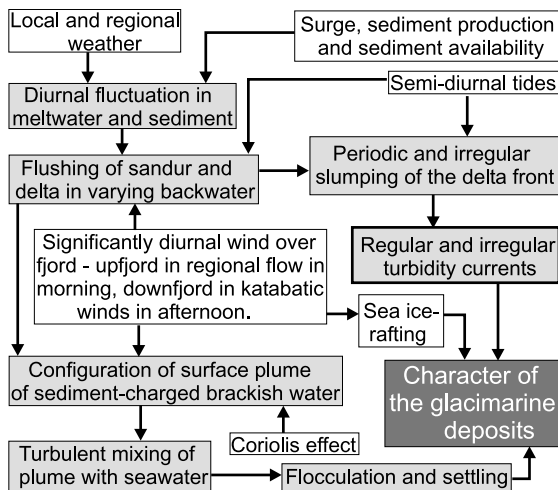


Fig. 13. Conceptual model of the processes controlling deposition of glacial sediment in Kuannersuit Sulluat. Shaded boxes represent responses to inputs, including those influenced by the surging glacier.

si-randomness of the ice-rafting and release processes. However, beyond 8 km downfjord, the concentration of IRD is significantly greater everywhere and there is little spatial trend, indicating lower rates of deposition of fine-grained sediment.

Beyond 8 km from the fjord head as represented by core D22 (Fig. 8), the fine-grained sediment is strongly bioturbated in all cores and organic contents are higher (6–8%). There is little or no lamination seen in visual examination or in the X-radiographs (GS and MS are more uniform than in proximal cores). Although the benthos was not specifically sampled in this study, several specimens of the mollusc, *Macoma calcarea*, were recovered from our small cores. The sediments are more fine-grained than those closer to the source with mean grain size about $4\ \mu\text{m}$ (Fig. 10). However, distributions are dominantly bimodal with a secondary peak in coarse silt and occasionally fine sand (<4%). There are no sandy layers in these sediments except for one poorly defined example in core D20. This is probably because (a) bioturbation and mechanical turbation by IRD mixes the sediment more effectively, and (b) this region is beyond the limit of all but the largest, least frequent gravity flow processes.

The cores cannot be dated except by inference

from the rates of accumulation in the traps (Fig. 5). Analysis of ^{137}Cs failed; activity was everywhere below detection. Based on accumulation data from the sediment traps, we infer that D4 (Fig. 8) represents 3 a of accumulation, D9 about 6 yr, and D14 about 40 a. Farther downfjord the rates are less certain but, based on the acoustic data, D22 may represent about 200 a.

6. Discussion

Gilbert et al. (1998) reported observations on the sedimentology of Kuannersuit Sulluat made from cores and CTDs recovered on 4 July 1995. The results shown in Fig. 2 indicate that the glacier began to surge sometime after 17 June 1995. Thus, although it had advanced about 1.2 km by 24 September and another 1.2 km in the next month, it is unlikely that the sediments in cores collected during that study contain a significant signal of the surge. So we are able to compare the sedimentary environment before and at the end of the 4 yr period of surging. Subsequent retreat of the glacier will probably continue to deliver greater than normal sediment loads for a number of years, both from the decaying ice itself and from the newly exposed landscape. Thus, although water discharge probably did not increase significantly as a result of surging (cf. Jaeger and Nittrouer, 1999a), sediment input has risen dramatically.

In the fjord the patterns of temperature and salinity in 2000 (this paper) and in 1997 (Desloges et al., 2002) are almost exactly as recorded at the beginning of the surge in 1995 (Gilbert et al., 1998), except for one notable difference: in 1995 the salinity of the fresh-water cap was 4–5‰, in 1997 8–9‰, and in 2000 15–20‰. We do not know if this is just an artifact of spot sampling that would be resolved by synoptic observations, but the increase is consistent and suggests more vigorous mixing of the overflowing cap with the sea water below. The increase in density due to SSC is relatively minor; the maximum observed in the river ($4\ \text{g l}^{-1}$) augments the density of fresh water at 4°C by $2.6\ \text{g l}^{-1}$, compared to the difference between fresh and brackish water immedi-

ately below the pycnocline of about 20 g l^{-1} . Nevertheless, it somewhat reduces the stability across the pycnocline, allowing for greater effect of mechanical mixing due to waves and interfacial shear. The anticipated impact is that more of the fine-grained sediment is deposited near the points of inflow, both as it is removed from transport by the outflowing cap and as flocculation and therefore accelerated settling (Hill et al., 1998) is more effective in the brackish cap and salt water beneath. The effect is that not only is more sediment delivered to the sea but a greater proportion is deposited proximally, doubly enhancing the probability of slope failures and the resultant generation of gravity flows.

Our earlier measurements did not reliably record SSC in the fjord, so it is not possible to compare by observation the occurrence of turbidity currents and related gravity flow processes. We do know from acoustic records taken in 1995 that the zone of ponded sediments representing gravity flow processes, especially turbidity currents, has a long history in the fjord with up to about 40 m of accumulation (Gilbert et al., 1998). We suggest that the region affected by these processes (Fig. 11) has advanced downfjord as the delta has prograded into the fjord, so that ponded sediments have progressively covered conformable sediments on the sea floor. However, we concluded, based on the rate of sediment accumulation, that even relatively minor gravity flow events that could be recognised in the cores had a recurrence interval of 30–50 a. Based on the sand layers in the cores, we suggest that the frequency has increased to 10 or more events per year.

The fine-grained components of the cores taken before (1995) and after (2000) the surge event are not greatly different. Colour, which varies from grey (2.5YR5/1, 5YR5/1) and very dark grey (2.5YR3/1, 5YR3/1) to olive (5Y4/3) and olive brown (2.5YR4/4) (Fig. 8), is characteristic of the volcanic rocks of the drainage basin. It is identical to the colour of the sediments deposited before the surge, which is not surprising, since the sediment sources are unchanged. The grain-size characteristics of the fine-grained sediment are also similar, with mean and median values generally less than $10 \mu\text{m}$ and very little sand content.

Again, this is expected given that much of this material is transported to the site through the water of the fjord where processes such as sorting and flocculation occur regardless of the input.

However, there are notable differences in the surge-generated sediments. The proximal sediments are more clearly laminated and layered in visual examination of the cores and as seen in the X-radiographs (see also Jaeger and Nittrouer, 1999a). These consist both of the subtle differences in the fine-grained sediments on a millimetre scale, and of the sand layers up to 8 cm thick representing more energetic processes (Ó Cofaigh and Dowdeswell, 2001). Both are a response to greater sediment input to the fjord. Also, a function of the greater input of fine-grained clastic materials from the river is the lower concentration of IRD on the fjord floor within 8 km of the delta and the lower organic carbon content of the sediments.

The most significant difference is in the rates of accumulation in the proximal region. Gilbert et al. (1998) and Desloges et al. (2002) calculated long-term rates of accumulation based on acoustic data and confirmed by ^{14}C dated cores of 9.5 mm a^{-1} 2 km from the head of the fjord (the site of T1), about 7 mm a^{-1} 4 km from the head (T2), and less than 5 mm a^{-1} 6 km from the head (T3). Thus, the rates recorded by the traps deployed in 2000 at the end of the glacial surge are 30 times, 27 times, and 6 times, respectively, the long-term averages. The rates of accumulation before the surge were comparable to those from fjords on East Greenland, Baffin Island and the Canadian High Arctic, although less than in fjords on Svalbard and in Kangerlussuaq, West Greenland, the latter fed directly from the inland ice of Greenland (Gilbert et al., 1998). But the rates in 2000 are among the highest in the world, except for the extremely active Alaskan fjords (Cowan and Powell, 1991), and are comparable to those in the glacial record of surges from the Bering Glacier, Alaska (Jaeger and Nittrouer, 1999a).

The questions of unequivocal recognition of surge-generated deposits in the glacial record and of distinguishing them from those of major hydroclimatically generated events (especially associated with floods due to intense precipitation

or glacial melt) are difficult to answer. Jaeger and Nittrouer (1999a) were able to document a record of six surging events in a century but at Kuannersuit Sulluat the effect is more subtle. It is limited to clear lamination of the sediments in response to discrete events (especially more turbidity currents generated by slumping of the delta front) in an environment of higher energy (Ó Cofaigh and Dowdeswell, 2001), and to significantly greater rates of accumulation that might only be recognised in ancient deposits by the absence of the other components of the sedimentary record (especially allochthonous organic matter and ice-rafted debris). Where surging has extended a glacier into the sea, the morphologic evidence (Solheim and Pfirman, 1985) should provide corroboration. At Kuannersuit Sulluat the surging glacier reached no closer than 10 km from the fjord head, and the terminus was well within the Little Ice Age moraine. Nevertheless, surging is a common phenomenon of glaciers and it is important to recognise that it does have an impact on the sedimentary record. The effect may appear similar to the imprint of other processes but useful palaeo-environmental assessment may depend on distinguishing them.

7. Conclusions

The processes influencing deposition of glacial-marine sediment in Kuannersuit Sulluat are summarised in Fig. 13. Before surging, sedimentary processes and deposits were determined principally by hydroclimatic and oceanic conditions and the interactions among them. The surging of a large glacier in the drainage basin had a marked effect on these components of the sedimentary environment of the fjord. Input of suspended fluvial sediment is significantly greater than before the surge event. Rates of sediment accumulation are up to 30 times greater than the long-term average before the surge, and rival rates in fjords with the greatest amounts of available sediment on Earth. Laminated fine-grained sediments deposited as a result of the spreading downfjord of the daily maximum of the inflow plume, compared to pre-surge sediments where

the rates of accumulation were too low for such events to be recognised. Thin beds of sandy turbidites from turbidity currents are generated about every 20 days during the melt season from the slope failures on the delta front, compared to these events generated on a scale of several decades before the surge. Concentrations of ice-rafted debris are very much reduced by the other overwhelmingly greater sources of sediment.

Each of these effects is limited to the immediate vicinity of the inflow. Turbidites deposited at about 20 day intervals within 2 km of the delta front are reduced to about one event per year within 4 km, even though acoustic data indicated that the largest events previously transported sediment 10 km downfjord.

Thus, close to the source there is a distinctive signal in the sedimentary record. This report does not follow the consequences of the surge to its conclusion when the glacier has retreated to its former size but it is anticipated that greater than normal sediment input will continue during the next several decades required for this to happen (Leonard, 1997), especially as landscape beneath the advanced glacier is revealed (cf. the concept of paraglacial sedimentation – Church and Ryder, 1972). During the full cycle of the surge (about 10 a) we anticipate that as much as 5 m of sediment or more may be deposited in the proximal environment, compared to 10–20 cm in the same period without surging. Whether the same sedimentary signal of laminated fine-grained sediment and sandy turbidites will occur throughout this period is not known, but this difference in accumulation is very much greater than could be anticipated from any single hydroclimatically controlled event or series of events in the drainage basin such as the rain-induced slope failure observed in the summer of 2000. It is also much greater than an increase in sedimentation that would occur from normal climatically induced glacial advance and retreat.

We do not know of previous surges in the drainage basin of Kuannersuit Sulluat, although the topographic map of the region suggests that a surge may have occurred earlier in the 20th century after and less extensively than the Little Ice Age maximum. Although the frequency of surging

glaciers may be decreasing elsewhere in the Arctic in response to climate warming (Dowdeswell et al., 1995), it is possible that this glacier may continue to surge intermittently in the future.

Acknowledgements

The study was supported by research and equipment grants from the Natural Sciences and Engineering Research Council of Canada, and from the Carlsberg Foundation. Captain Jorgen Broberg and the crew of *Porsild* worked with cheerful good will to make the field programme possible. Mansour Khazaali and Will Junkin assisted in the laboratory and office. Thoughtful reviews were provided by Ellen Cowan and Colm Ó Cofaigh.

References

- Beierle, B.D., Lamoureux, S.F., Cockburn, J.M.H., Spooner, I., 2002. A new method for visualizing sediment particle size distributions. *J. Paleolimnol.* 27, 279–283.
- Bornhold, B.D., Ren, P., Prior, D.B., 1994. High-frequency turbidity currents in British Columbia fjords. *Geomar. Lett.* 14, 238–243.
- Church, M., Ryder, J.M., 1972. Paraglacial sedimentation: a consideration of fluvial processes conditioned by glaciation. *Geol. Soc. Am. Bull.* 83, 3059–3072.
- Cowan, E.A., Cai, J., Powell, R.D., Seramur, K.C., Spurgeon, V.L., 1998. Modern tidal rhythmites deposited in a deep-water estuary, southeast Alaska. *Geomar. Lett.* 18, 40–48.
- Cowan, E., Seramur, K.C., Cai, J., Powell, R.D., 1999. Cyclic sedimentation produced by fluctuations in meltwater discharge, tides and marine productivity in an Alaskan fjord. *Sedimentology* 46, 1109–1126.
- Cowan, E.A., Powell, R.D., 1991. Ice-proximal sediment accumulation rates in a temperate glacial fjord, southeastern Alaska. In: Anderson, B.J., Ashley, G.M. (Eds.), *Glacial Marine Sedimentation; Paleoclimatic Significance*. Geological Society of America Special Paper 261, pp. 61–73.
- Desloges, J.R., Gilbert, R., Nielsen, N., Christiansen, C., Rasch, M., Øhlenschläger, R., 2002. Holocene sedimentary environments in fiords of Disko Bugt, West Greenland. *Quat. Sci. Rev.* 21, 947–963.
- Dowdeswell, J.A., Hamilton, G.S., Hagen, J.O., 1991. The duration of the active phase on surge-type glaciers: contrasts between Svalbard and other regions. *J. Glaciol.* 37, 388–399.
- Dowdeswell, J.A., Hodgkins, R., Nuttall, A.M., 1995. Mass-balance change as a control on the frequency and occurrence of glacier surges in Svalbard, Norwegian High Arctic. *Geophys. Res. Lett.* 22, 2909–2912.
- Gilbert, R., 1982. Contemporary sedimentary environments on Baffin Island, N.W.T., Canada: glaciomarine processes in fiords of eastern Cumberland Peninsula. *Arct. Alp. Res.* 14, 1–12.
- Gilbert, R., 1983. Sedimentary processes of Canadian arctic fjords. *Sediment. Geol.* 36, 147–175.
- Gilbert, R., 2000. Environmental assessment from the sedimentary record of high latitude fiords. *Geomorphology* 32, 295–314.
- Gilbert, R., Nielsen, N., Desloges, J.R., Rasch, M., 1998. Contrasting glaciomarine sedimentary environments of two arctic fiords on Disko, West Greenland. *Mar. Geol.* 147, 63–83.
- Hill, P.S., Syvitski, J.M., Cowan, E.A., Powell, R.D., 1998. In situ observations of floe settling velocities in Glacier Bay, Alaska. *Mar. Geol.* 145, 85–94.
- Jaeger, J.M., Nittrouer, C.A., 1999a. Marine record of surge-induced outburst floods from the Bering Glacier, Alaska. *Geology* 27, 847–850.
- Jaeger, J.M., Nittrouer, C.A., 1999b. Sediment deposition in an Alaskan Fjord: controls on the formation and preservation of sedimentary structures in Icy Bay. *J. Sediment. Res.* 69, 1011–1026.
- Leonard, E.M., 1997. The relationship between glacial activity and sediment production: evidence from a 4450-year varve record of neoglacial sedimentation at Hector Lake, Alberta, Canada. *J. Paleolimnol.* 17, 319–330.
- Lewis, T., Gilbert, R., Lamoureux, S.F., 2002. Spatial and temporal changes in sedimentary processes at high-arctic proglacial Bear lake, Devon Island, Nunavut, Canada. *Arct. Antarct. Alp. Res.* 34, 119–129.
- Mackiewicz, N.E., Powell, R.D., Carlson, P.R., Molnia, B.F., 1984. Interlaminated ice-proximal glaciomarine sediments in Muir Inlet, Alaska. *Mar. Geol.* 57, 113–147.
- Meier, M.F., Post, A.S., 1969. What are glacier surges? *Can. J. Earth Sci.* 6, 807–819.
- Middleton, G.V., 1966. Experiments in density and turbidity currents II. Uniform flow of density currents. *Can. J. Earth Sci.* 3, 627–637.
- Ó Cofaigh, C., Dowdeswell, J.A., 2001. Laminated sediments in glaciomarine environments: diagnostic criteria for their interpretation. *Quat. Sci. Rev.* 20, 1411–1436.
- Ó Cofaigh, C., Dowdeswell, J.A., Grobe, H., 2001. Holocene-glaciomarine sedimentation, inner Scoresby Sund, East Greenland: the influence of fast-flowing ice-sheet outlet glaciers. *Mar. Geol.* 175, 103–129.
- Raymond, C.F., 1987. How do glaciers surge? A review. *J. Geophys. Res.* 92, 9121–9134.
- Sharp, M.J., 1988. Surging glaciers: geomorphic effects. *Prog. Phys. Geogr.* 12, 533–559.
- Solheim, A., Pfirman, S.L., 1985. Sea-floor morphology outside a grounded, surging glacier: Bråsellbreen, Svalbard. *Mar. Geol.* 65, 127–143.
- Syvitski, J.P.M., Burrell, D.C., Skei, J.M., 1987. *Fjords Processes and Products*. Springer, New York.